ACKNOWLEDGMENT

The author thanks D. Véron for constant support and P. Belland for helpful discussions. Excellent technical assistance from P. Gaudin is also gratefully acknowledged.

REFERENCES

[1] J. Shmoys, "Proposed diagnostic method for cylindrical plasma," *J. Appl. Phys.*, vol. 32, pp. 689–695, Apr. 1961.
[2] C. Etiévant, "Les méthodes de mesure pour l'étude du plasma du Tokamak TFR," Rep. EUR-CEA-FC-764, Feb. 1975.
[3] Equipe TFR, "Diagnostics employés sur le Tokamak TFR," Rep. EUR-CEA-FC-877, Jan. 1977.
[4] D. Véron, J. Certain, and J. P. Crenn, "Multichannel HCN interferometer for electron density profile measurements of Tokamak plasmas," *J. Opt. Soc. Amer.*, vol. 67, pp. 964–967, July 1977.
[5] J. P. Crenn, "Etude de l'utilisation de la propagation guidée pour l'interférométrie infrarouge sur les Tokamaks," Rep. EUR-CEA-FC-924, Nov. 1977.
[6] D. J. Kroon, *Spectroscopic Techniques for Far Infrared Submillimeter and Millimeter Waves*. Amsterdam, The Netherlands: D. H. Martin, 1967, ch. 7, pp. 310–380.
[7] A. Doswell and D. J. Harris, "Modified *H* guide for millimeter and submillimeter wavelengths," *IEEE Trans. Microwave Theory Tech.*, vol. MTT-21, pp. 587–589, Sept. 1973.
[8] R. J. Batt, H. L. Bradley, A. Doswell, and D. J. Harris, "Waveguide and open-resonator techniques for submillimeter waves," *IEEE Trans. Microwave Theory Tech.*, vol. MTT-22, pp. 1089–1094, Dec. 1974.
[9] E. A. J. Marcatili, R. A. Schmeltzer, "Hollow metallic and dielectric waveguides for long distance optical transmission and lasers," *Bell. Syst. Tech. J.*, vol. 43, pp. 1783–1808, July 1964.
[10] J. R. Birch, R. J. Cook, A. F. Harding, R. G. Jones, and G. D. Price, "The optical constants of ordinary glass from 0.29 to 4000 cm^{-1}," *J. Phys. D: Appl. Phys.*, vol. 8, pp. 1353–1358, Apr. 1975.
[11] H. Krammer, "Field configurations and propagation constants of modes in hollow rectangular dielectric waveguides," *IEEE J. Quantum Electron.*, vol. QE-12, pp. 505–506, Aug. 1976.
[12] J. J. Degnan, "The waveguide laser: A review," *Appl. Phys.*, vol. 11, pp. 1–33, 1976.
[13] M. Yamanaka, "Optically pumped waveguide lasers," *J. Opt. Soc. Amer.*, vol. 67, pp. 952–958, July 1977.
[14] F. K. Kneubühl, "Waveguides for submillimeter-wave lasers," *J. Opt. Soc. Amer.*, vol. 67, pp. 959–963, July 1977.
[15] P. Belland, C. Pigot, and D. Véron, "Pocket size CW HCN waveguide laser," *Phys. Lett.*, vol. 56A, pp. 21–22, Feb. 1976.
[16] P. Belland, D. Véron, and L. B. Whitbourn, "Scaling laws for CW 0.337 mm HCN waveguides lasers," *Appl. Opt.*, vol. 15, pp. 3047–3053, Dec. 1976.
[17] J. L. Bruneau, "Lasers submillimétriques continus compacts HCN ($\lambda = 0.337$ mm) et DCN ($\lambda \approx 0.195$; 0.190 mm)," Rep. EUR-CEA-FC-898, June 1977.
[18] J. J. Degnan, "Waveguide laser mode patterns in the near and far field," *Appl. Opt.*, vol. 12, pp. 1026–1030, May 1973.
[19] D. R. Hall, E. K. Gorton, and R. M. Jenkins, "10-μm propagation losses in hollow dielectric waveguides," *J. Appl. Phys.*, vol. 48, pp. 1212–1216, Mar. 1977.
[20] P. Belland, D. Véron, and L. B. Whitbourn, "Mode study, beam characteristics and output power of a CW 0.337 mm HCN waveguide laser," *J. Phys. D: Appl. Phys.*, vol. 8, pp. 2113–2123, 1975.
[21] R. L. Abrams, "Coupling losses in hollow waveguide laser resonators," *IEEE J. Quantum Electron*, vol. QE-8, pp. 838–843, Nov. 1972.

An Exact Three-Dimensional Field Theory for a Class of Cyclic *H*-Plane Waveguide Junction

RAY J. COPPLESTONE

***Abstract*—The device analyzed consists of g waveguides meeting in a cavity with a central metal disk. A conducting boundary such as this occurs in practical waveguide-junction circulators and the technique developed here may find application in circulator field theory. A special case of the geometry considered here is the 'tuning screw' which arises when $g = 2$.**

The method of analysis is by representing the fields by mode summation, in the usual way, and then matching to the metal surfaces and across various imaginary internal boundaries. The device is assumed lossless.

The agreement between experimental and theoretical results is very good, thus indicating the method is valid and has been formulated correctly.

Manuscript received February 13, 1978; revised August 4, 1978.

The author is with the Hirst Research Centre, the General Electric Company, Ltd., Wembley, England.

I. INTRODUCTION

UNTIL RECENTLY there had been little work published regarding complete three-dimensional field theories of waveguide junctions with application to circulator geometry. Davies [1] in 1962 and El-Shandwily *et al.* [2] in 1973 produced theories for *H*-plane circulators with variation confined to the *H*-plane. Recently a method was formulated for handling some of the three-dimensional problems occurring in an *E*-plane waveguide-junction circulator geometry [3].

An *H*-plane circulator design may assume the form of a full height ferrite cylinder standing on a metal disk

0018-9480/79/0600-0577$00.75 ©1979 IEEE

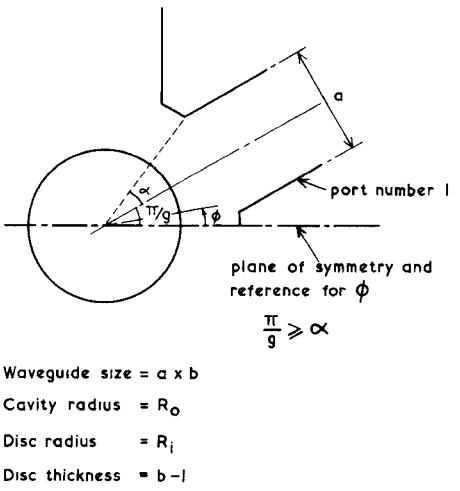

Fig. 1. General geometry of the cyclic H-plane g-port waveguide junction with central metal disk.

located centrally in the junction. The metal boundary of such a circulator is given in Fig. 1, and defines the device considered in this paper. The junction cavity is a true cavity whose radius R_0 is a parameter. All other authors appear to have considered junctions in which the waveguides intersect each other; i.e., for a cyclic g-port a fixed cavity radius of $a/(2\sin\pi/g)$ would have been used.

There are two main boundaries across which field-matching takes place; these are the coordinate surfaces of radii R_0 and R_i (the disk radius). On the inner side of the radius R_0 there is dielectric (air) only, but on the outer side there are both dielectric and metal. This considerably complicates the process of matching the fields between the waveguides and the cavity compared with that of reference [1]. At the dielectric–dielectric part of the interface the tangential components of both the electric and magnetic fields are matched, but at the dielectric–metal part only the tangential electric field is matched, i.e., set to zero. The same principle is employed at the disk step at the boundary of radius R_i. The disk gives the problem a three-dimensional nature, and field variation in the direction of the junction axis (z-axis) must be taken into account throughout the whole junction, including the waveguides. The resulting problem, even without the ferrite, is considerably more complicated than the two-dimensional ferrite-loaded junction dealt with previously. This paper does not treat the theory for the ferrite-loaded or the ferrite-loaded and p-i-n-loaded junctions, but the author has found that such an extension of the theory is relatively straightforward compared with the problem of the metal boundary.

Referring to Fig. 1, the disk radius is made to satisfy the condition

$$R_i < R_0\left(1-(a/(2R_0))^2\right)^{1/2} \tag{1}$$

in order that the matching interface of radius R_0 will belong to the rectangular-cross-section portion of the waveguides as well as to the cavity. This implies that for the case of the limiting cavity, defined by intersecting waveguides, the upper bound for R_i for $g=3$ would be $a\sqrt{3}/6$. This would be a restriction in the application to circulators and is one reason for using a true cavity.

Thus the method of analysis involves solving Maxwell's equations in three dimensions for the waveguides, the outer cavity ($R_0 \geqslant r \geqslant R_i$), and the inner cavity ($R_i \geqslant r \geqslant 0$), and matching the tangential fields at the coordinate surfaces of radii R_0 and R_i. The resulting equations are manipulated to lead to a set of linear equations whose unknowns are the complex mode amplitudes for the waveguides and inner cavity. The device is assumed lossless and the theory includes no approximations other than the usual truncation of infinite series for computational purposes.

II. Waveguide Fields

The waveguide is defined in Fig. 2, together with the coordinate axes. In the usual way, the time dependence is assumed to be given by $\exp\{j\omega t\}$. Solving Maxwell's equations for the incident and scattered dominant mode and all of the scattered evanescent modes, the following expressions are obtained:

$$E_x = \sum_{p=1}^{\infty}\sum_{q=1}^{\infty} B_{pq}\sin\frac{p\pi y}{a}\sin\frac{q\pi z}{b}\exp\{-\gamma_{pq}x\} \tag{2}$$

$$E_y = \sum_{p=0}^{\infty}\sum_{q=1}^{\infty} -A_{pq}\frac{q\pi}{b}\frac{j\omega\mu_0}{k(p,q)}\cos\frac{p\pi y}{a}\cdot\sin\frac{q\pi z}{b}\exp\{-\gamma_{pq}x\} + \sum_{p=1}^{\infty}\sum_{q=1}^{\infty} -B_{pq}\frac{p\pi}{a}\frac{\gamma_{pq}}{k(p,q)}\cdot\cos\frac{p\pi y}{a}\sin\frac{q\pi z}{b}\exp\{-\gamma_{pq}x\} \tag{3}$$

$$E_z = \frac{-j\omega\mu_0}{\pi/a}\sin\frac{\pi y}{a}\left(A\exp\{j\gamma_{10}x\}+A_{10}\exp\{-j\gamma_{10}x\}\right) + \sum_{\substack{p=1\\(p,q)\neq(1,0)}}^{\infty}\sum_{q=0}^{\infty} -A_{pq}\frac{p\pi}{a}\frac{j\omega\mu_0}{k(p,q)}\sin\frac{p\pi y}{a}\cos\frac{q\pi z}{b}\cdot\exp\{-\gamma_{pq}x\} + \sum_{p=1}^{\infty}\sum_{q=1}^{\infty} -B_{pq}\frac{q\pi}{b}\frac{\gamma_{pq}}{k(p,q)}\sin\frac{p\pi y}{a}\cdot\cos\frac{q\pi z}{b}\exp\{-\gamma_{pq}x\} \tag{4}$$

$$H_x = \cos\frac{\pi y}{a}\left(A\exp\{j\gamma_{10}x\}+A_{10}\exp\{-j\gamma_{10}x\}\right) + \sum_{\substack{p=0\\(p,q)\neq(0,0)\\\neq(1,0)}}^{\infty}\sum_{q=0}^{\infty} A_{pq}\cos\frac{p\pi y}{a}\cos\frac{q\pi z}{b}\exp\{-\gamma_{pq}x\} \tag{5}$$

$$H_y = \frac{-j\gamma_{10}}{\pi/a}\sin\frac{\pi y}{a}\left(A\exp\{j\gamma_{10}x\}-A_{10}\exp\{-j\gamma_{10}x\}\right) + \sum_{\substack{p=1\\(p,q)\neq(1,0)}}^{\infty}\sum_{q=0}^{\infty} A_{pq}\frac{p\pi}{a}\frac{\gamma_{pq}}{k(p,q)}\sin\frac{p\pi y}{a}\cos\frac{q\pi z}{b}\exp\{-\gamma_{pq}x\} + \sum_{p=1}^{\infty}\sum_{q=1}^{\infty} B_{pq}\frac{q\pi}{b}\frac{j\omega\epsilon_0}{k(p,q)}\sin\frac{p\pi y}{a}\cos\frac{q\pi z}{b}\exp\{-\gamma_{pq}x\} \tag{6}$$

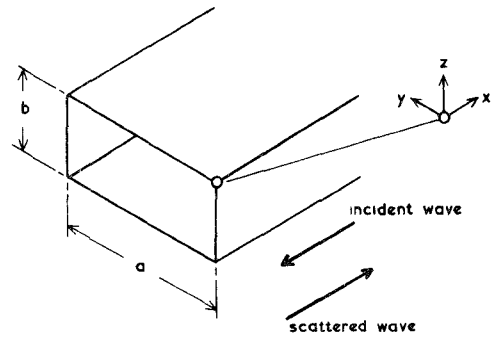

Fig. 2. Waveguide convention. The plane $x=0$ is the internal phase-reference plane.

$$H_z = \sum_{p=0}^{\infty}\sum_{q=1}^{\infty} A_{pq}\frac{q\pi}{b}\frac{\gamma_{pq}}{k(p,q)}\cos\frac{p\pi y}{a}\sin\frac{q\pi z}{b}\cdot\exp\{-\gamma_{pq}x\} + \sum_{p=1}^{\infty}\sum_{q=1}^{\infty} -B_{pq}\frac{p\pi}{a}\frac{j\omega\epsilon_0}{k(p,q)}\cos\frac{p\pi y}{a}\cdot\sin\frac{q\pi z}{b}\exp\{-\gamma_{pq}x\} \tag{7}$$

where

$$k(p,q)=(p\pi/a)^2+(q\pi/b)^2 \tag{8}$$

$$\gamma_{pq}=|\{k(p,q)-\omega^2\mu_0\epsilon_0\}^{1/2}|, \qquad (p,q)\neq(0,0). \tag{9}$$

The time dependent factor has been omitted. The A_{pq} and B_{pq} define the amplitudes of the TE_{pq} and TM_{pq} modes. Only the TE_{10} mode propagates, all other modes being evanescent. The amplitude of the incident dominant mode is defined by A.

III. Cavity Fields

The cavity regions and the cylindrical coordinate system are defined in Fig. 3. In this section a general formulation is presented for the fields in such regions. Introducing the magnetic Hertzian vector potential [4], $\bar{\Pi}_h$

$$\bar{E} = -j\omega\mu_0\nabla\times\bar{\Pi}_h \tag{10}$$

$$\bar{H} = \nabla\times\nabla\times\bar{\Pi}_h \tag{11}$$

$$(\nabla^2+k_0^2)\bar{\Pi}_h = 0, \qquad k_0^2=\omega^2\mu_0\epsilon_0. \tag{12}$$

Then, setting $\bar{\Pi}_h=\Pi_h\hat{z}$ for the TE modes ($E_z=0$), equation (12) can be solved for Π_h and subsequently all field components follow from (10) and (11). A similar procedure can be adopted for the TM-modes by introducing the electric Hertzian vector potential $\bar{\Pi}_e$. The general mode fields for a cylindrical region of height h are then as follows.

TM_{0n} modes:

$$E_r = 0 \tag{13}$$

$$E_\phi = 0 \tag{14}$$

$$E_z = k_0^2\left[C_{0n}J_n(k_0r)+D_{0n}H_n^{(1)}(k_0r)\right]\exp\{jn\phi\} \tag{15}$$

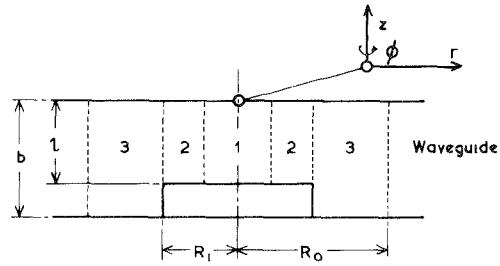

Fig. 3. Numbering of regions of cavity.

$$H_r = \frac{-\omega\epsilon_0 n}{r}\left[C_{0n}J_n(k_0r)+D_{0n}H_n^{(1)}(k_0r)\right]\exp\{jn\phi\} \tag{16}$$

$$H_\phi = -j\omega\epsilon_0 k_0\left[C_{0n}J_n'(k_0r)+D_{0n}H_n^{(1)'}(k_0r)\right]\exp\{jn\phi\} \tag{17}$$

$$H_z = 0. \tag{18}$$

TM_{mn} modes ($m\neq 0$):

$$E_r = \frac{-jm\pi k_m}{h}\left[C_{mn}j^{n-1}I_n'(k_mr)+D_{mn}\frac{2}{\pi}j^{-n-2}K_n'(k_mr)\right]\cdot\sin\frac{m\pi z}{h}\exp\{jn\phi\} \tag{19}$$

$$E_\phi = \frac{-jmn\pi}{hr}\left[C_{mn}j^{n}I_n(k_mr)+D_{mn}\frac{2}{\pi}j^{-n-1}K_n(k_mr)\right]\cdot\sin\frac{m\pi z}{h}\exp\{jn\phi\} \tag{20}$$

$$E_z = -k_m^2\left[C_{mn}j^{n}I_n(k_mr)+D_{mn}\frac{2}{\pi}j^{-n-1}K_n(k_mr)\right]\cdot\cos\frac{m\pi z}{h}\exp\{jn\phi\} \tag{21}$$

$$H_r = \frac{-\omega\epsilon_0 n}{r}\left[C_{mn}j^{n}I_n(k_mr)+D_{mn}\frac{2}{\pi}j^{-n-1}K_n(k_mr)\right]\cdot\cos\frac{m\pi z}{h}\exp\{jn\phi\} \tag{22}$$

$$H_\phi = \omega\epsilon_0 k_m\left[C_{mn}j^{n-1}I_n'(k_mr)+D_{mn}\frac{2}{\pi}j^{-n-2}K_n'(k_mr)\right]\cdot\cos\frac{m\pi z}{h}\exp\{jn\phi\} \tag{23}$$

$$H_z = 0. \tag{24}$$

TE_{mn} modes ($m\neq 0$):

$$E_r = \frac{\omega\mu_0 n}{r}\left[A_{mn}j^{n}I_n(k_mr)+B_{mn}\frac{2}{\pi}j^{-n-1}K_n(k_mr)\right]\cdot\sin\frac{m\pi z}{h}\exp\{jn\phi\} \tag{25}$$

$$E_\phi = -\omega\mu_0 k_m\left[A_{mn}j^{n-1}I_n'(k_mr)+B_{mn}\frac{2}{\pi}j^{-n-2}K_n'(k_mr)\right]\cdot\sin\frac{m\pi z}{h}\exp\{jn\phi\} \tag{26}$$

$$E_z = 0 \tag{27}$$

$$H_r = \frac{jm\pi k_m}{h}\left[A_{mn}j^{n-1}I_n'(k_mr)+B_{mn}\frac{2}{\pi}j^{-n-2}K_n'(k_mr)\right]\cdot\cos\frac{m\pi z}{h}\exp\{jn\phi\} \tag{28}$$

$$H_\phi = \frac{jmn\pi}{hr}\left[A_{mn}j^n I_n(k_m r) + B_{mn}\frac{2}{\pi}j^{-n-1}K_n(k_m r)\right] \cdot\cos\frac{m\pi z}{h}\exp\{jn\phi\} \tag{29}$$

$$H_z = -k_m^2\left[A_{mn}j^n I_n(k_m r) + B_{mn}\frac{2}{\pi}j^{-n-1}K_n(k_m r)\right] \cdot\sin\frac{m\pi z}{h}\exp\{jn\phi\}. \tag{30}$$

In (13)–(30), $J_n(x)$ is the Bessel function of the first kind, $H_n^{(1)}(x)$ is a Hankel function, and $I_n(x)$ and $K_n(x)$ are modified Bessel functions [5]. Also, $k_m = \sqrt{|k_0^2 - (m\pi/h)^2|}$, where h is the height of the region ($h=b$ or $h=l$).

IV. Simplification of Notation

In order to simplify the field-matching procedure, the following notation for the cavity-field expressions is introduced:

$$\begin{aligned}
\alpha_{mn11} &= -\omega\mu_0 k_m j^{n-1} I_n'(k_m r_i)\\
\alpha_{mn12} &= -\omega\mu_0 k_m j^{-n-2}\frac{2}{\pi}K_n'(k_m r_i)
\end{aligned} \tag{31}$$

$$\begin{aligned}
\alpha_{mn13} &= \frac{-jmn\pi}{hr_i}j^n I_n(k_m r_i)\\
\alpha_{mn14} &= \frac{-jmn\pi}{hr_i}j^{-n-1}\frac{2}{\pi}K_n(k_m r_i)
\end{aligned} \tag{32}$$

$$\begin{aligned}
\alpha_{mn21} &= 0\\
\alpha_{mn22} &= 0
\end{aligned} \tag{33}$$

$$\begin{aligned}
\alpha_{mn23} &= -k_m^2 j^n I_n(k_m r_i)\\
\alpha_{mn24} &= -k_m^2 j^{-n-1}\frac{2}{\pi}K_n(k_m r_i)
\end{aligned} \tag{34}$$

$$\begin{aligned}
\alpha_{mn31} &= \frac{jmn}{hr_i}\pi j^n I_n(k_m r_i)\\
\alpha_{mn32} &= \frac{jmn}{hr_i}\pi\frac{2}{\pi}j^{-n-1}K_n(k_m r_i)
\end{aligned} \tag{35}$$

$$\begin{aligned}
\alpha_{mn33} &= \omega\epsilon_0 k_m j^{n-1} I_n'(k_m r_i)\\
\alpha_{mn34} &= \omega\epsilon_0 k_m\frac{2}{\pi}j^{-n-1}K_n'(k_m r_i)
\end{aligned} \tag{36}$$

$$\begin{aligned}
\alpha_{mn41} &= -k_m^2 j^n I_n(k_m r_i)\\
\alpha_{mn42} &= -k_m^2\frac{2}{\pi}j^{-n-1}K_n(k_m r_i)
\end{aligned} \tag{37}$$

$$\begin{aligned}
\alpha_{mn43} &= 0\\
\alpha_{mn44} &= 0.
\end{aligned} \tag{38}$$

The radius r_i is an inner cylindrical-boundary radius. A set of parameters β_{mnij} is similarly defined for an outer cylindrical boundary. Equations (13)–(30) can now be united and summed over all mode numbers to yield the following equations for the tangential fields on an inner cylindrical boundary:

$$E_\phi = \sum_{m=1}^{\infty}\sum_{n=-\infty}^{\infty}(\alpha_{mn11}A_{mn} + \alpha_{mn12}B_{mn} + \alpha_{mn13}C_{mn} + \alpha_{mn14}D_{mn})\sin\frac{m\pi z}{h}\exp\{jn\phi\} \tag{39}$$

$$E_z = \sum_{m=0}^{\infty}\sum_{n=-\infty}^{\infty}(\alpha_{mn23}C_{mn} + \alpha_{mn24}D_{mn})\cos\frac{m\pi z}{h}\cdot\exp\{jn\phi\} \tag{40}$$

$$H_\phi = \sum_{m=0}^{\infty}\sum_{n=-\infty}^{\infty}(\alpha_{mn31}A_{mn} + \alpha_{mn32}B_{mn} + \alpha_{mn33}C_{mn} + \alpha_{mn34}D_{mn})\cos\frac{m\pi z}{h}\exp\{jn\phi\} \tag{41}$$

$$H_z = \sum_{m=1}^{\infty}\sum_{n=-\infty}^{\infty}(\alpha_{mn41}A_{mn} + \alpha_{mn42}B_{mn})\sin\frac{m\pi z}{h}\cdot\exp\{jn\phi\}. \tag{42}$$

Replacement of the α's by the β's leads to similar sets of equations for the tangential fields on an outer boundary. For the purpose of matching region-3 to the waveguides, parameters a, b, c, and d are introduced as follows.

$$a_{mn}^{(3)} = \beta_{mn11}^{(3)}A_{mn}^{(3)} + \beta_{mn12}^{(3)}B_{mn}^{(3)} + \beta_{mn13}^{(3)}C_{mn}^{(3)} + \beta_{mn14}^{(3)}D_{mn}^{(3)} \tag{43}$$

$$b_{mn}^{(3)} = \beta_{mn23}^{(3)}C_{mn}^{(3)} + \beta_{mn24}^{(3)}D_{mn}^{(3)} \tag{44}$$

$$c_{mn}^{(3)} = \beta_{mn31}^{(3)}A_{mn}^{(3)} + \beta_{mn32}^{(3)}B_{mn}^{(3)} + \beta_{mn33}^{(3)}C_{mn}^{(3)} + \beta_{mn34}^{(3)}D_{mn}^{(3)} \tag{45}$$

$$d_{mn}^{(3)} = \beta_{mn41}^{(3)}A_{mn}^{(3)} + \beta_{mn42}^{(3)}B_{mn}^{(3)} \tag{46}$$

where superscript (3) refers to the region. Similarly for the region-2–region-3 interface,

$$e_{mn}^{(2)} = \beta_{mn11}^{(2)}A_{mn}^{(2)} + \beta_{mn12}^{(2)}B_{mn}^{(2)} + \beta_{mn13}^{(2)}C_{mn}^{(2)} + \beta_{mn14}^{(2)}D_{mn}^{(2)} \tag{47}$$

$$f_{mn}^{(2)} = \beta_{mn23}^{(2)}C_{mn}^{(2)} + \beta_{mn24}^{(2)}D_{mn}^{(2)} \tag{48}$$

$$g_{mn}^{(2)} = \beta_{mn31}^{(2)}A_{mn}^{(2)} + \beta_{mn32}^{(2)}B_{mn}^{(2)} + \beta_{mn33}^{(2)}C_{mn}^{(2)} + \beta_{mn34}^{(2)}D_{mn}^{(2)} \tag{49}$$

$$h_{mn}^{(2)} = \beta_{mn41}^{(2)}A_{mn}^{(2)} + \beta_{mn42}^{(2)}B_{mn}^{(2)} \tag{50}$$

$$e_{mn}^{(3)} = \alpha_{mn11}^{(3)}A_{mn}^{(3)} + \alpha_{mn12}^{(3)}B_{mn}^{(3)} + \alpha_{mn13}^{(3)}C_{mn}^{(3)} + \alpha_{mn14}^{(3)}D_{mn}^{(3)} \tag{51}$$

$$f_{mn}^{(3)} = \alpha_{mn23}^{(3)}C_{mn}^{(3)} + \alpha_{mn24}^{(3)}D_{mn}^{(3)} \tag{52}$$

$$g_{mn}^{(3)} = \alpha_{mn31}^{(3)}A_{mn}^{(3)} + \alpha_{mn32}^{(3)}B_{mn}^{(3)} + \alpha_{mn33}^{(3)}C_{mn}^{(3)} + \alpha_{mn34}^{(3)}D_{mn}^{(3)} \tag{53}$$

$$h_{mn}^{(3)} = \alpha_{mn41}^{(3)}A_{mn}^{(3)}\alpha_{mn42}^{(3)}B_{mn}^{(3)}. \tag{54}$$

V. Matching Region-2 to Region-3

Using expressions of the type shown in (39)–(42) for the fields at the region-2–region-3 interface, and employing the notation defined in (47)–(54), the matching procedure leads to the following equations:

$$e_{fn}^{(2)}=\frac{2}{l}\sum_{m=1}^{\infty}\frac{-(-1)^m m}{\pi b}\sin\frac{f\pi b}{l}\frac{e_{mn}^{(3)}}{(m/b)^2-(f/l)^2} \tag{55}$$

$$f_{0n}^{(2)}=\frac{b}{l}f_{0n}^{(3)} \tag{56}$$

$$f_{fn}^{(2)}=\frac{2}{l}\sum_{m=0}^{\infty}\frac{-(-1)^m f}{\pi l}\sin\frac{f\pi b}{l}\frac{f_{mn}^{(3)}}{(m/b)^2-(f/l)^2} \tag{57}$$

$$g_{0n}^{(2)}=2g_{0n}^{(3)}+\frac{2}{l}\sum_{m=1}^{\infty}\frac{b}{m\pi}\sin\frac{m\pi l}{b}g_{0n}^{(3)} \tag{58}$$

$$g_{fn}^{(2)}=\frac{2}{l}\sum_{m=0}^{\infty}\frac{(-1)^f m}{\pi b}\sin\frac{m\pi l}{b}\frac{g_{mn}^{(3)}}{(m/b)^2-(f/l)^2} \tag{59}$$

$$h_{fn}^{(2)}=\frac{2}{l}\sum_{m=1}^{\infty}\frac{(-1)^f f}{\pi l}\sin\frac{m\pi l}{b}\frac{h_{mn}^{(3)}}{(m/b)^2-(f/l)^2}. \tag{60}$$

The values taken by n are discussed in Section VI; here they are simply defined thus: $n=gk+\nu$, where g is the number of waveguide ports, $\nu=0,1,\cdots,g-1$, and $k=0,\pm1,\pm2,\cdots$. For computational purposes the infinite series expressions for the fields are truncated. Thus the maximum values for f, k, and m are F, K, and M.

For a given value of n a column vector for the region-2 coefficients appearing on the left-hand side of (55)–(60) is defined as

$$(f_{0n}^{(2)}g_{0n}^{(2)}e_{1n}^{(2)}f_{1n}^{(2)}g_{1n}^{(2)}h_{1n}^{(2)}e_{2n}^{(2)}\cdots h_{Fn}^{(2)})'. \tag{61}$$

Now let such vectors for $k=0$, $k=1$, $k=-1$, $k=2,\cdots$ be strung together to form a column vector of all of the e's, f's, g's, and h's of the outer boundary of region-2, and denote the vector by $\{efgh(2)\}'$. Similarly

$$(f_{0n}^{(3)}\cdots h_{Mn}^{(3)})' \tag{62}$$

is defined for the inner boundary of region-3, and such vectors are strung together to form a vector denoted by $\{efgh(3)\}'$. Now the elements of $\{efgh(2)\}'$ and $\{efgh(3)\}'$ are related according to (56)–(60), which may be written in the compact form

$$\{efgh(2)\}'=\mathbf{W}\{efgh(3)\}' \tag{63}$$

where $\mathbf{W}$ is a nonsquare 'block diagonal' matrix of size $2(2K+1)(2F+1)\times2(2K+1)(2M+1)$. The blocks are identical and of size $2(2F+1)\times2(2M+1)$.

Now let the A's, B's, C's, and D's of the region-2 be formed into a vector exactly corresponding to $\{efgh(2)\}'$. This involves simply changing e to A, etc., giving $\{ABCD(2)\}'$. The elements of these two vectors are related according to (47)–(50) and, therefore, a matrix $\mathbf{Z}_0^{(2)}$ is defined for the outer boundary of region-2 so that

$$\{efgh(2)\}'=\mathbf{Z}_0^{(2)}\{ABCD(2)\}'. \tag{64}$$

The matrix is square, of order $2(2K+1)(2F+2)$, and block diagonal. Each block is of order $(4F+2)$ and is also block diagonal with a leading block of order 2 and F blocks of order 4. Similarly

$$\{efgh(3)\}'=\mathbf{Z}_i^{(3)}\{ABCD(3)\}' \tag{65}$$

where $\mathbf{Z}_i^{(3)}$ is the square block diagonal matrix of order $2(2K+1)(2M+1)$ for the inner boundary of region-3. The elements of the matrix are the coefficients in (51)–(54).

Finally, (63)–(65) are combined to give

$$\mathbf{Z}_0^{(2)}\{ABCD(2)\}'=\mathbf{W}\mathbf{Z}_i^{(3)}\{ABCD(3)\}'. \tag{66}$$

Premultiplication by $\mathbf{Z}_0^{(2)-1}$ can be performed to express the mode amplitudes of region-2 in terms of those of region-3. However, this will not be done here because there is no region-1 and $\mathbf{Z}_0^{(2)}$ needs special treatment. This will be discussed in Section VII.

VI. Cyclic Boundary Conditions

In this section, a technique used by Davies [1] is employed. Since the junction under consideration is cyclic with a g-fold axis, then the scattering matrix $[S]$ is cyclic and of order g. Its eigenvectors are, therefore, given by

$$\bar{x}_\nu=\frac{1}{\sqrt{g}}\left(\exp\left\{\frac{j2\pi\nu}{g}\right\},\quad\exp\left\{\frac{j4\pi\nu}{g}\right\},\cdots,1\right) \tag{67}$$

and the corresponding eigenvalues, λ_ν, satisfy

$$\mathbf{S}\bar{x}_\nu=\lambda_\nu x_\nu,\qquad \nu=0,1,\cdots,(g-1). \tag{68}$$

Referring to Fig. 1, let $\psi(\phi,z)$ for $0<\phi\leqslant2\pi/g$, $-b\leqslant z\leqslant0$, and $r=R_0$, denote a tangential field quantity over the first arc of the region-3 boundary $r=R_0$. That part of the arc satisfying $\pi/g-\alpha<\phi<\pi/g+\alpha$ is inside port number 1.

Now, all of the ports are driven simultaneously with the same input power but with different phases. The relative phases are given by the components of an eigenvector; thus the junction is driven with 'eigenvector excitation.' The boundary condition at $r=R_0$ is, therefore,

$$\text{1st arc:}\quad \psi[\phi,z] \qquad 0<\phi\leqslant\frac{2\pi}{g},\ -b\leqslant z\leqslant0 \tag{69}$$

$$\text{2nd arc:}\quad \psi\left[\phi-\frac{2\pi}{g},z\right]\exp\left\{\frac{j2\pi\nu}{g}\right\} \qquad \frac{2\pi}{g}<\phi\leqslant\frac{4\pi}{g},\ -b\leqslant z\leqslant0 \tag{70}$$

$$g\text{th arc:}\quad \psi\left[\phi-\frac{2\pi}{g}(g-1),z\right]\exp\left\{\frac{j2\pi\nu}{g}(g-1)\right\} \qquad \frac{2\pi}{g}(g-1)<\phi\leqslant2\pi,\ -b\leqslant z\leqslant0. \tag{71}$$

Let the complete function specified by (69)–(71) be denoted by Ψ and let superscripts (3) and (w) denote the cavity side and waveguide side of the boundary. Then, matching, orthogonalizing with respect to ϕ, and using

(69)–(71), it is easily shown that

$$\int_0^{2\pi} \Psi^{(3)} \exp\{-jn'\phi\}\, d\phi$$
$$= g\int_0^{2\pi/g} \Psi^{(w)}[\phi, z] \exp\{-jn'\phi\}\, d\phi, \qquad n' = gk' + \nu$$
$$= 0, \qquad \text{for other } n' \tag{72}$$

where $k' = 0, \pm 1, \pm 2, \cdots, \pm K$. This result shows that with eigenvector excitation, it is only necessary to match at one waveguide port. Also, the cavity region contains only those modes for which the mode number n is equal to $\nu(\text{mod } g)$.

VII. Matching Region-3 to the Waveguides

From (39)–(46) the tangential field components on the boundary $r = R_0$ of region-3 are given by

$$E_\phi^{(3)} = \sum_{m=1}^{M} \sum_{k=-K}^{M} a_{mn}^{(3)} \sin\frac{m\pi z}{b} \exp\{jn\phi\} \tag{73}$$

$$E_z^{(3)} = \sum_{m=0}^{M} \sum_{k=-K}^{M} b_{mn}^{(3)} \cos\frac{m\pi z}{b} \exp\{jn\phi\} \tag{74}$$

$$H_\phi^{(3)} = \sum_{m=0}^{M} \sum_{k=-K}^{M} c_{mn}^{(3)} \cos\frac{m\pi z}{b} \exp\{jn\phi\} \tag{75}$$

$$H_z^{(3)} = \sum_{m=1}^{M} \sum_{k=-K}^{M} d_{mn}^{(3)} \sin\frac{m\pi z}{b} \exp\{jn\phi\}. \tag{76}$$

Then, matching region-3 to the waveguides with the aid of (72),

$$\frac{\pi b}{g} a_{mn'}^{(3)} = \int_{-b}^{0}\int_{(\pi/g)-\alpha}^{(\pi/g)+\alpha} E_\phi^{(w)} \sin\frac{m\pi z}{b} \exp\{-jn'\phi\}\, d\phi\, dz \tag{77}$$

$$\frac{2\pi b}{g} b_{0n'}^{(3)} = \int_{-b}^{0}\int_{(\pi/g)-\alpha}^{(\pi/g)+\alpha} E_z^{(w)} \exp\{-jn'\phi\}\, d\phi\, dz \tag{78}$$

$$\frac{\pi b}{g} b_{mn'}^{(3)} = \int_{-b}^{0}\int_{(\pi/g)-\alpha}^{(\pi/g)+\alpha} E_z^{(w)} \cos\frac{m\pi z}{b} \exp\{-jn'\phi\}\, d\phi\, dz \tag{79}$$

$$2b\alpha \sum_{k=-K}^{K} c_{0n}^{(3)} (-1)^{k-k'} \frac{\sin g(k-k')\alpha}{g(k-k')\alpha} = \int_{-b}^{0}\int_{(\pi/g)-\alpha}^{(\pi/g)+\alpha} H_\phi^{(w)} \exp\{-jn'\phi\}\, d\phi\, dz \tag{80}$$

$$b\alpha \sum_{k=-K}^{K} c_{mn}^{(3)} (-1)^{k-k'} \frac{\sin g(k-k')\alpha}{g(k-k')\alpha} = \int_{-b}^{0}\int_{(\pi/g)-\alpha}^{(\pi/g)+\alpha} H_\phi^{(w)} \cos\frac{m\pi z}{b} \exp\{-jn'\phi\}\, d\phi\, dz \tag{81}$$

$$b\alpha \sum_{k=-K}^{K} d_{mn}^{(3)} (-1)^{k-k'} \frac{\sin g(k-k')\alpha}{g(k-k')\alpha} = \int_{-b}^{0}\int_{(\pi/g)-\alpha}^{(\pi/g)+\alpha} H_z^{(w)} \sin\frac{m\pi z}{b} \exp\{-jn'\phi\}\, d\phi\, dz. \tag{82}$$

The a's, b's, c's, and d's appearing on the left-hand side of (77)–(82) can be assembled to form the vector $\{abcd(3)\}'$, and then $\mathbf{X}$ is the matrix defined such that $\mathbf{X}\{abcd(3)\}'$ is the column vector whose elements are the left-hand sides of these equations. For the right-hand sides a column sub-vector is defined:

$$\int_{-b}^{0}\int_{(\pi/g)-\alpha}^{(\pi/g)+\alpha} \left(E_z^{(w)}, H_\phi^{(w)}, E_\phi^{(w)} \sin\frac{\pi z}{b}, E_z^{(w)} \cos\frac{\pi z}{b}, H_\phi^{(w)} \cos\frac{\pi z}{b}, H_z^{(w)} \sin\frac{\pi z}{b}, \cdots, H_z^{(w)} \sin\frac{M\pi z}{b}\right)' \cdot \exp\{-jn'\phi\}\, d\phi\, dz \tag{83}$$

then taking all such vectors for $k' = 0, 1, -1, \cdots, K$, and $-K$, a vector $\bar{V}$ may be formed. Equations (77)–(82) may now be expressed in the compact form

$$\mathbf{X}\{abcd(3)\}' = \bar{V}. \tag{84}$$

The matrix is of order $2(2K+1)(2M+1)$. Similar to $\mathbf{Z}_0^{(2)}$ in (64), a matrix $\mathbf{Z}_0^{(3)}$ is defined for the outer boundary of region-3 so that (43)–(46) may be written

$$\{abcd(3)\}' = \mathbf{Z}_0^{(3)}\{ABCD(3)\}' \tag{85}$$

The matrix is of order $2(2K+1)(2F+1)$. Equations (66), (84), and (85) may be combined to yield

$$\mathbf{Z}_0^{(2)}\{ABCD(2)\}' = \mathbf{W}\mathbf{Z}_i^{(3)}\mathbf{Z}_0^{(3)\,-1}\mathbf{X}^{-1}\bar{V}. \tag{86}$$

The procedure for determining $\bar{V}$ is as follows. Since matching takes place across arcs on the circle $r = R_0$, the waveguide fields in (2)–(7) must be expressed in polar coordinates. Thus on the boundary,

$$x = R_0\left[\cos\left(\phi - \frac{\pi}{g}\right) - \cos\alpha\right] \tag{87}$$

$$y = R_0 \sin\left(\phi - \frac{\pi}{g}\right) + \frac{a}{2} \tag{88}$$

$$E_\phi^{(w)} = E_y^{(w)} \cos\left(\phi - \frac{\pi}{g}\right) - E_x^{(w)} \sin\left(\phi - \frac{\pi}{g}\right) \tag{89}$$

$$H_\phi^{(w)} = H_y^{(w)} \cos\left(\phi - \frac{\pi}{g}\right) - H_x^{(w)} \sin\left(\phi - \frac{\pi}{g}\right). \tag{90}$$

It can now be shown that $\bar{V}$, of which (83) is a sub-vector, may be expressed in the form

$$\bar{V} = \mathbf{Y}\bar{M} \tag{91}$$

where $\mathbf{Y}$ is a matrix of size $2(2K+1)(2M+1) \times \{P+1+Q(2P+1)\}$ and $\bar{M}$ is the column vector of waveguide mode amplitudes A_{pq}, B_{pq}, with P and Q as the maximum values of p and q. The vector $\bar{M}$ is formed from the following sequence of $(Q+1)$ vectors:

$$(A, A_{10}, \cdots, A_{P0})' \tag{92}$$
$$(A_{01}, A_{11}, \cdots, A_{P1}, B_{11}, \cdots, B_{P1})' \tag{93}$$
$$- - - - - - - - - - - - - - - - - -$$
$$(A_{0Q}, A_{1Q}, \cdots, A_{PQ}, B_{1Q}, \cdots, B_{PQ})'. \tag{94}$$

From (86) and (91),

$$\mathbf{Z}_0^{(2)}\{ABCD(2)\}' = \mathbf{W}\mathbf{Z}_i^{(3)}\mathbf{Z}_0^{(3)\,-1}\mathbf{X}^{-1}\mathbf{Y}\bar{M}. \quad (95)$$

This equation contains all of the mode amplitudes for the waveguides and for region-2. In the case considered in this paper there is no region-1 and, therefore, the region-2 field equations must not include Bessel functions with poles at the origin. Therefore, in (95) alternate columns of $\mathbf{Z}_0^{(2)}$, starting with the second column, are deleted. The corresponding alternate elements of $\{ABCD(2)\}'$ are also deleted. Then, the right-hand side of (95) is moved to the left-hand side to form the equation

$$(\bar{r}\,\mathbf{R})[c/C] = [0] \quad (96)$$

where $\bar{r}$ is a column vector, $\mathbf{R}$ a matrix, c a single element, and $\bar{C}$ is the column vector of all scattered waveguide mode amplitudes and central region-2 mode amplitudes, and [0] is a null column vector, all of appropriate size. Now $c = A$, the dominant waveguide mode amplitude for the incident wave, and is defined to be unity at $x = 0$, the phase reference plane. Thus

$$\mathbf{R}\bar{C} = -\bar{r}. \quad (97)$$

The number of equations here is $2(2K+1)(2F+1)$, and the number of unknowns is $(2K+1)(2F+1)+P+Q(2P+1)$. Taking

$$Q = M \leqslant P = 2K+1 \quad (98)$$

there is a deficiency of M equations, therefore, M of the TM mode amplitudes are set to zero:

$$B_{pQ} = 0 \qquad p = P-M+1, P-M+2, \cdots, P. \quad (99)$$

Equations (97) and (99) can now be solved together for the mode amplitudes, in particular the scattered dominant mode amplitude A_{10}. Now since $A = 1$, then A_{10} is the reflection coefficient. Furthermore since eigenvector excitation is being used, then

$$A_{10} = \lambda_\nu. \quad (100)$$

VIII. Experimental and Theoretical Results

Theoretical and experimental eigenvalues have been determined for four designs, viz., a two-port junction with and without a central metal disk, and a three-port junction with and without a central metal disk. The devices are specified in Figs. 4 and 5. The device in Fig. 4 has the configuration of a tuning screw in a waveguide with slight indentations.

The experimental results were obtained by making slotted line measurements at one port only, using matched load and/or fixed short-circuit terminations at the other ports. The results were used to calculate the experimental eigenvalues. A necessary condition for a lossless device is $|\lambda_\nu| = 1$. All of the theoretical results satisfied the condition $||\lambda_\nu| - 1| \not> 0.001$, and it was found that usually $|\lambda_\nu| = 1.000000$. Experimental eigenvalues were ~ 0.97 in magnitude, this low value being consistent with loss in the measurement system. The phases of the experimental and theoretical eigenvalues over X band are plotted in Fig. 6. The phase references for the eigenvalues are defined in Figs. 4 and 5.

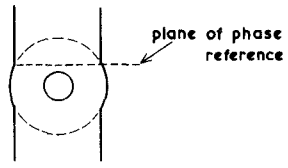

Waveguide size	22·86 x 10·16 mm²
Cavity radius	12·4 mm
Disc radius	3·5mm
Disc thickness	3·0mm

Fig. 4. Experimental cyclic 2-port junction: 'tuning-screw' geometry.

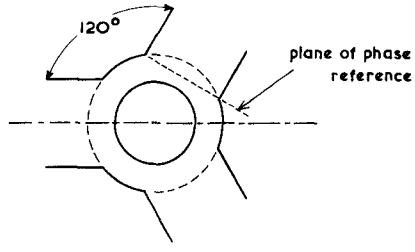

Waveguide size	22·86 x 10·16 mm²
Cavity radius	18·0mm
Disc radius	10·0mm
Disc thickness	3·0mm

Fig. 5. Experimental cyclic 3-port junction.

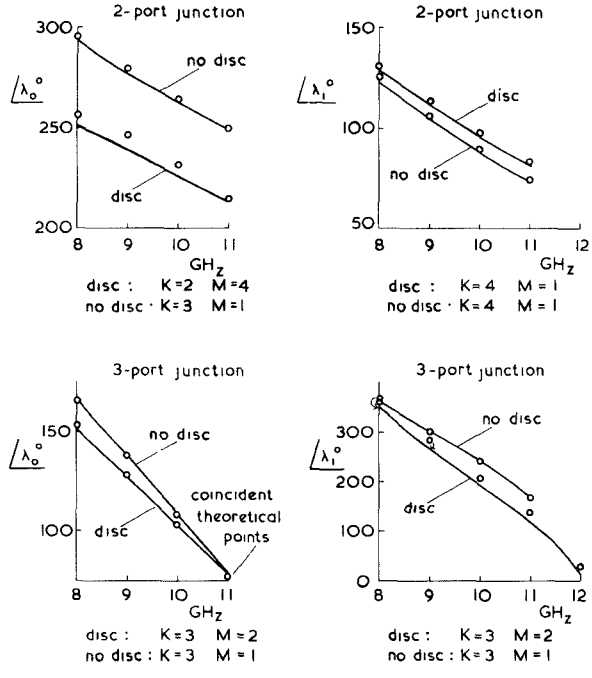

Fig. 6. Experimental (—) and theoretical (o) eigenvalue phases for the two-port and three-port of Figs. 4 and 5, with and without the central metal disk.

The results shown in the figure are the best obtained for these particular designs. Discrepancy between theory and experiment is expected because i) the theory does not account for loss, ii) the method of obtaining the experimental eigenvalues from the measurements assumes there is no loss, and iii) only a finite number of modes is included (e.g., for λ_0 for the 2-port with a disk, $K=2$, $M=4$ means that the azimuthal spacial frequencies accounted for are 0, ± 2, ± 4 ($= \pm gK$), and in the z-direction modes with up to four half-wavelengths are included). However, the correlation is very good.

For the 2-port case it is seen that the disk has a greater influence on λ_0 than on λ_1. This is to be expected since the disk is of small radius and the stationary (for λ_0) and the rotating (for λ_1) junction modes have high and low electric fields near the junction center. For the 3-port the disk has little effect on λ_0. This suggests the edge of the disk is in a region of low electric field. Indeed, the disk and no-disk cases give the same result at 11 GHz and it is found that the first root of $J_0(\omega\sqrt{\mu_0\epsilon_0}\, r)$ gives the result $r = 10.4$ mm: the disk radius is 10.0 mm. For the rotating junction made the dominant field mode Bessel function, J_1, is near a maximum for the whole frequency band at the disk edge. This means that the electric field is high and, therefore, a high value of M is required for accurate results. It is, therefore, not surprising that errors as large as 22° occur in this case. Also, this particular eigenvalue is degenerate, i.e., $\lambda_1 = \lambda_2$, and numerical errors are expected in such cases [1], although the results for the case of no-disk are very good.

IX. Conclusions

An exact three-dimensional field theory has been formulated for a class of cyclic H-plane waveguide junction, and a small number of designs have been briefly evaluated to test the theory. The accuracy of the results is very good, thus indicating the theory is valid and has been programmed correctly. The problem solved here has involved the organization of a large number of linear simultaneous equations with the aid of matrix notation. The inclusion of extra dielectric or ferrite regions can be achieved by defining the appropriate matrices and including them in the matrix product occurring in the theory. Additional metal disks can also be included by introducing the appropriate matrices. Thus the method developed in this paper represents a principle for dealing with a multistep pedestal, multidielectric, multiferrite-loaded junction, with or without a central metal pin.

References

[1] J. B. Davies, "An analysis of the m-port symmetrical H-plane waveguide junction with central ferrite post," *IRE Trans. Microwave Theory Tech.*, vol. MTT-10, pp. 596–604, Nov. 1962.

[2] M. E. El-Shandwily *et al.*, "General field theory treatment of H-plane waveguide junction circulators," *IEEE Trans. Microwave Theory Tech.*, vol. MTT-21, pp. 392–403, June 1973.

[3] ——, "General field theory treatment of E-plane waveguide junction circulators–Part II: Two-disk ferrite configuration," *IEEE Trans. Microwave Theory Tech.*, vol. MTT-25, pp. 794–803, Sept. 1977.

[4] J. A. Stratton, *Electromagnetic Theory*. New York: McGraw-Hill, 1941.

[5] M. Abramowitz and I. A. Stegun, *Handbook of Mathematical Functions*, Dover, New York, 1965.

On the Modeling of the Edge-Guided Mode Stripline Isolators

SALVADOR H. TALISA, MEMBER, IEEE, AND DONALD M. BOLLE, SENIOR MEMBER, IEEE

***Abstract*—A model for the inhomogeneously ferrite-loaded microstrip and stripline is considered. The structure consists of a loaded ferrite slab between two infinite, perfectly conducting planes with the bias magnetization perpendicular to the ground planes. The ferrite is taken to be lossy and is loaded on one side by a semi-infinite lossy material and on the other by a dielectric slab. The modal spectrum of this configuration as well as the influence on the ω-α and ω-β diagrams of the various parameters involved are studied. Special attention has been paid to the capabilities of this configuration to model a nonreciprocal isolator. A hypothetical isolator is designed, and its characteristics are compared with experimental results obtained by Hines, Dydyk, and Courtois. Substantial agreement is observed.**

Manuscript received July 10, 1978; revised December 6, 1978.

The authors are with the Division of Engineering, Brown University, Providence, RI 02912.

I. Introduction

An investigation of edge-guided waves propagating in ferrite-loaded strip and microstriplines magnetized perpendicular to the ground plane was initiated by Hines [1]–[3] in the late 1960's. Hines deduced that the dominant mode propagating through such struc-

0018-9480/79/0600-0584$00.75 ©1979 IEEE